sciendo

Slovak Journal of Civil Engineering

Vol. 32, 2024, No. 3, 1 –12
DOI: 10.2478/sjce-2024-0014

NON-UNIFORM TORSION BEHAVIOR OF THIN-WALLED BEAMS ACCORDING TO THE FINITE ELEMENT METHOD

Dang-Bao TRAN[1*]

Abstract

This study is based on a theory for analyzing non-uniform torsion in thin-walled beams made of homogeneous elastic material with arbitrary cross-sections by incorporating the effect of the shear deformation of a cross-section. Utilizing the Finite Element Method (FEM), the proposed numerical approach addresses non-uniform torsion by breaking down a 3D analysis into 2D cross-sectional and 1D modeling components. Initially, the geometric constants of the cross-section were computed using a 9-node isoparametric element in 2D FEM. Subsequently, a 1D FEM employing a linear isoparametric element calculated the twist angle, torsion warping parameters, and stress results. The stress field was determined through a local analysis of the 2D cross-section. Notably, the 2D FEM component aligns with contemporary trends in commercial software, thereby bolstering the potential and practical applicability of the proposed numerical approach. Its verification and validation through numerical analyses using MATLAB underscore the efficacy and reliability of the method in analyzing non-uniform torsion behavior in structural design, particularly under diverse boundary conditions.

Address

[1] Dept. of Civil Engineering, Faculty of Architecture, Thu Dau Mot University, Tran Van On 06, Thu Dau Mot City, Binh Duong Province, Vietnam

[*] ***Corresponding author:*** baotd@tdmu.edu.vn

Key words

- Non-uniform torsion,
- Structural design,
- Shear deformation,
- Thin-walled structures,
- Vlasov's theory,
- Warping.

1 INTRODUCTION

Torsion is a common concern in the design of thin-walled beams. Saint-Venant's theory (Timoshenko and Goodier, 1970; Pilkey, 2002) deals with the stress field of a prismatic beam with homogeneous isotropic material when any cross-section warping is not constrained. This theory has been extensively studied in (Grutmman et al., 1999; Tran et al., 2021; Tran, 2021).

However, in practical structural design, the cross-sectional warping of thin-walled beams is often limited by boundary conditions and geometric constraints, which can cause additional normal and shear stresses that are not accounted for in Saint-Venant's theory. To address this issue, Vlasov proposed a theory of non-uniform torsion in 1940 (Vlasov, 1961), which assumes that the shear strain in the middle surface of thin-walled beams is negligible. As a result, the axial displacement depends on the derivative of the twist angle and the warping function.

The applicability of Vlasov's theory is limited to open cross-sections, as it can result in significant errors when applied to closed cross-sections where the shear stresses are distributed along the perimeter of the cross-section without altering their direction across a thin wall's thickness (Saadé et al., 2004). Benscoter's torsion theory (1954), accounts for shear deformation and differs from Vlasov's approach by incorporating a dimensionless parameter in the axial displacement field rather than relying on the twist angle rate. As a result, Benscoter's theory provides more accurate stress field predictions for closed cross-sections, as demonstrated by Shakourzadeh et al. (1995).

Many researchers have developed FEM models that consider non-uniform torsion and account for the effects of shear deformation. Tralli (1986) developed a hybrid model to investigate the stress and strain of thin-walled beams with arbitrary cross-sections. Shakourzadeh et al. (1995) proposed a hyperbolic interpolation-based FEM model to analyze torsional problems in both open and closed cross-sections using Benscoter's theory. Prokić (1993, 1996) proposed a novel warping function considering non-uniform torsion in arbitrary cross-sections. This function varies linearly between adjacent nodal points, which are created by dividing the cross-section's midline according to accuracy needs. Back and Will (1998) developed a shear-flexible element by combining Vlasov's and Timoshenko's beam theories for general cross-sections.

Kim and Kim (2005) developed a 14 x 14 matrix by introducing a displacement field and applying the Hellinger–Reissner principle (Braess, 2007) to account for the effect of shear forces and restrained warping torsion on shear deformation in thin-walled beams. Erkmen et al. (2006) used FEM to analyze torsion that incorporates shear deformation by applying the principle of stationary complementary energy and assuming an admissible stress field.

Murín et al. (2008, 2012, 2014) enhanced the standard beam elements of a stiffness matrix from 12 x 12 to 14 x 14 by incorporating additional degrees of freedom, particularly the torsion angle derivative induced by the bi-moment. Unlike Vlasov's theory, which defines this parameter by the entire twist angle derivative (Vlasov, 1961), Murín's modified approach specifically addresses the effects of deformation-induced secondary torque. Significantly, Murin et al. (2021, 2022) and Fotiu and Murin (2021) have developed advanced beam theories for functionally graded material, which is particularly well-suited for analyzing non-uniform torsion in homogeneous materials.

El Fatmi (2007) proposed a beam theory by introducing three warping parameters to describe the warping function caused by torsion and shear force, which account for non-uniformity resulting from bending and torsion. Genoese et al. (2013) developed a mixed finite element approach that addresses the Saint-Venant stress field by introducing independent warping parameters and applying the Hellinger–Reissner principle. Ferradi et al. (2013) developed a FEM that effectively accounts for normal stress resulting from restrained torsion by expressing cross-sectional warping as a linear combination of warping modes. Addessi et al. (2021) introduced an approach for examining non-uniform torsion in thin-walled structures. This method involves the introduction of three warping parameters distributed along the length of a beam, and the warping parameter of the 2D cross-section is deduced through the utilization of 2D Lagrange polynomials (Wunderlich and Pilkey, 2002). Lewiński (2021) developed a novel first-order warping function that incorporated elements of existing theories, such as those offered by Vlasov (1961), Kim and Kim (2005), El Fatmi (2007), Librescu and Song (2005), Timoshenko (1921), and Timoshenko (1922), to construct a comprehensive theory of straight elastic bars.

The stress field resulting from kinematical assumptions, as explored by El Fatmi (2007) and Lewiński and Czarnecki (2021), was utilized without correction, leading to a violation of a longitudinal local equilibrium equation due to the inadequate representation of shear stresses, as pointed out by Genoese et al. (2013). Ferradi et al. (2013) proposed an indirect correction by incorporating several higher warping modes multiplied by independent warping parameters to address this issue. Although this approach converges to the actual solution, it increases the number of degrees of freedom and complicates the formulation. Tsipiras and Sapountzakis (2014) applied the boundary element method (BEM), known for its exclusive discretization needs within the boundary region (Wunderlich and Pilkey, 2002) to account for the secondary effect of torsional shear deformation. Their theoretical framework systematically integrates the fundamental principles expressed by Genoese et al. (2013) and Ferradi et al. (2013).

The stress fields in thin-walled beams subjected to non-uniform torsion have not been adequately addressed in commercial software. Even when they are considered, errors may persist (Murín and Kutiš, 2008). Engineers commonly rely on 1D elements in linear beam analysis, followed by a section analysis incorporating material nonlinearity. Even widely used softwares, such as SAP2000 and SCIA, which employ a 12 x 12 stiffness matrix for beam elements, does not provide internal forces resulting from non-uniform torsion in beams. Using shell or solid elements for a stress analysis is less flexible and computationally efficient than the superimposition technique, 2D cross-sections, and 1D beam element approaches.

To the best of the author's knowledge, two distinct methodologies have been employed in homogeneous materials for determining warping on cross-sections. The first method relies on Lagrange interpolation functions to establish pre-oriented points within the cross-section, as demonstrated in the research conducted by Addessi et al. (2021). The second approach involves a 2D Finite Element discretization of the element's cross-sections, requiring the solution of an elliptical differential equation. Notably, the latter methodology has found practical application in programming for commercial software packages such as IDEA StatiCa, Allplan Bridge (based on Grutmman et al., 1999), and SCAD (based on Fialko, 2013).

The methodology proposed by Tsipiras and Sapountzakis (2014) holds significant promise for addressing non-uniform torsion in homogeneous materials. However, their study utilizing the BEM has limitations in demonstrating practical applications. In addition to these limitations and despite the growing acknowledgment of BEM as a competitor to the FEM (Paradiso et al., 2020), major global structural analysis software companies continue to prioritize FEM.

This study aims to present a numerical technique utilizing FEM to address non-uniform torsion, while considering shear deformation in thin-walled beams with a consistent arbitrary cross-section made of homogeneous isotropic elastic material. The proposed approach is grounded in the well-established theory of Tsipiras and Sapountzakis (2014). The FEM-derived method will be illustrated by exploring its application for non-uniform torsion analysis. A 2D FEM based on the Galerkin approach (Zienkiewicz and Taylor, 2000) has been developed by solving an elliptical differential equation governing the warping function. Significantly, this warping approach aligns with the prevailing trend in commercial software, rendering it a promising choice for practical applications. The remaining kinematic variables of the beam are derived through the principle of virtual work, which is implemented using a 1D FEM.

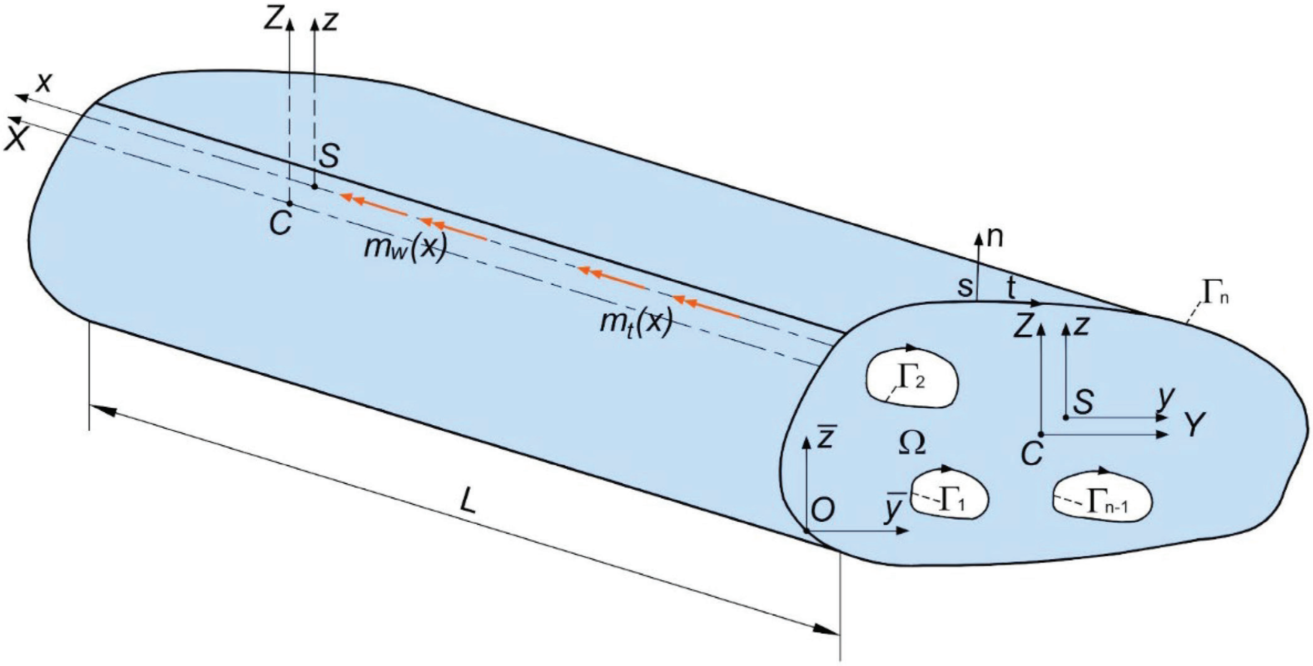

Fig. 1 *Illustration of Cross-Sectional Shape and Torsional Loading on a Prismatic Beam*

2 METHODS

2.1 Incorporating Shear Deformation in Non-uniform Torsion Formulas: A Brief Overview

The main objective of the current research is to analyze a beam with a cross-section that maintains a constant shape throughout its length L and is composed of a homogeneous isotropic elastic material with a modulus of elasticity E and shear modulus G. Fig. 1 illustrates the longitudinal axis of the beam, which is the x-axis, and the cross-sectional plane is positioned on the $y - z$ plane. The cross-section's shear center, denoted as S, is detailed in construction procedures outlined in Grutmman et al. (1999). The intersection of the parallel system $\bar{z}=z + z_s$ and $\bar{y}=y + y_s$ is designated as point O. Furthermore, a parallel system with $Sxyz$ is defined as $CXYZ$, with C symbolizing the center of gravity.

The domain Ω with multiple connectivities is enclosed by n curves, Γ_1 , Γ_2 ,..., Γ_{n-1} , and Γ_n. The tangent vector t and its corresponding coordinate s, as well as the normal vector n, establish a right-handed system. The beam is subjected to various types of loads, including a distributed warping moment $M_w(x)$, distributed torque $M_t(x)$, concentrated warping moment $M_{wi}(x)$, and concentrated torque $M_{ti}(x)$, while the cross-section is assumed to experience no deformation.

$$\begin{aligned} u(x,y,z) &= \theta_x^{'}\phi_S^P(y,z),\\ v(x,z) &= -z\theta_x(x),\\ w(x,y) &= y\theta_x(x), \end{aligned} \tag{1}$$

Eq. (1) as presented in this study, represents the axial displacement as a function of the torsion angle derivative and the warping function. Vlasov proposed this equation for evaluating non-uniform torsion in open thin-walled cross-section bars (Vlasov, 1961). However, his theory did not consider the impact of shear deformation on restrained torsional warping. The omission of this factor is inadequate for analyzing non-uniform torsion in closed cross-sections, as demonstrated by Murín and Kutiš (2008) and Mokos and Sapountzakis (2011).

In contrast, Benscoter's theory (Benscoter, 1954) considers both the effect of shear deformation and a dimensionless parameter in the axial displacement field, thereby providing a more comprehensive approach for predicting the stress field in closed cross-sections. Eq. (2) expresses the displacement field proposed by Benscoter's theory:

$$\begin{aligned} u(x,y,z) &= \eta_x\phi_S^P(y,z),\\ v(x,z) &= -z\theta_x(x),\\ w(x,y) &= y\theta_x(x), \end{aligned} \tag{2}$$

where *u, v and w* are the axial and transverse displacements of the beam concerning $Sxyz$:

θ_x is the twist angle

η_x is the torsion warping parameter

$\phi_S^P(y,z)$, is the primary torsional warping function for shear center S determined by:

$$\begin{aligned} &\nabla^2\phi_S^P = 0 \text{ in } \Omega\\ &\frac{\partial\phi_S^P}{\partial y}n_y + \frac{\partial\phi_S^P}{\partial z}n_z = zn_y - yn_z \text{ on } \Gamma_n. \end{aligned} \tag{3}$$

Additionally, the primary torsional warping function can be achieved through coordinate transformation, as suggested by Gruttmann et al. (1999):

$$\phi_S^P(y,z) = \left(\phi_O^P(\bar{y},\bar{z}) - \frac{1}{A}\int_\Omega \phi_O^P(\bar{y},\bar{z})dA\right) + \bar{y}_S Z - \bar{z}_S Y, \tag{4}$$

where $\phi_O^P(\bar{y},\bar{z})$ is the primary torsional warping function concerning the $O(\bar{y},\bar{z})$ system coordinates. The area of the cross-section is represented by the symbol A.

The strain associated with the displacement field in Eq. (2) can be represented as:

$$\begin{aligned} \varepsilon_{xx} &= \eta_x' \phi_S^P, \\ \gamma_{xy} &= \underbrace{\theta_x'\left(\frac{\partial \phi_S^P}{\partial y} - z\right)}_{\gamma_{xy}^P} + \underbrace{\left(\eta_x - \theta_x'\right)\frac{\partial \phi_S^P}{\partial y}}_{\gamma_{xy}^S}, \\ \gamma_{xz} &= \underbrace{\theta_x'\left(\frac{\partial \phi_S^P}{\partial z} + y\right)}_{\gamma_{xz}^P} + \underbrace{\left(\eta_x - \theta_x'\right)\frac{\partial \phi_S^P}{\partial z}}_{\gamma_{xz}^S}. \end{aligned} \tag{5}$$

The stress field arising from the strain in Eq. (5) is expressed as follows:

$$\sigma_{xx} = E\varepsilon_{xx} = E\eta_x'\phi_S^P, \tag{6}$$

$$\begin{aligned} \tau_{xy} = G\gamma_{xy} &= \underbrace{G\theta_x'\left(\frac{\partial \phi_S^P}{\partial y} - z\right)}_{\tau_{xy}^P} + \underbrace{G\left(\eta_x - \theta_x'\right)\frac{\partial \phi_S^P}{\partial y}}_{\tau_{xy}^S}, \\ \tau_{xz} = G\gamma_{xz} &= \underbrace{G\theta_x'\left(\frac{\partial \phi_S^P}{\partial z} + y\right)}_{\tau_{xz}^P} + \underbrace{G\left(\eta_x - \theta_x'\right)\frac{\partial \phi_S^P}{\partial z}}_{\tau_{xz}^S}. \end{aligned} \tag{7}$$

The principle of virtual work, excluding volumetric forces, is utilized to derive the global equilibrium equations:

$$\begin{aligned} &\int_V \left(\sigma_{xx}\delta\varepsilon_{xx} + \tau_{xy}\delta\gamma_{xy} + \tau_{xz}\delta\gamma_{xz}\right)dV = \\ &= \int_F \left(t_x\delta u + t_y\delta v + t_z\delta w\right)dF \end{aligned} \tag{8}$$

where

$\delta(.)$ denotes the virtual quantities

t_x, t_y, t_z represent components of the traction vector

V denotes the volume

F represents the surface area of the bar, including the cross sections of the end.

The warping moment (M_w), primary twisting moment (M_t^P), secondary twisting moment (M_t^S), and total twisting moment (M_t) are represented by the symbols mentioned. The following mathematical expressions define these quantities:

$$\begin{aligned} M_w &= -\int_\Omega \left(\sigma_{xx}\phi_S^P\right)d\Omega, \\ M_t^P &= \int_\Omega \left[\tau_{xy}^P\left(\frac{\partial \phi_S^P}{\partial y} - z\right) + \tau_{xz}^P\left(\frac{\partial \phi_S^P}{\partial z} + y\right)\right]d\Omega, \\ M_t^S &= -\int_\Omega \left[\tau_{xy}^S\frac{\partial \phi_S^P}{\partial y} + \tau_{xz}^S\frac{\partial \phi_S^P}{\partial z}\right]d\Omega, \\ M &= M_t^P + M_t^S. \end{aligned} \tag{9}$$

By inserting Eqs. (6) and (7) into the left side of Eq. (8), the resultant stress in Eq. (9) can be expressed in an alternative form:

$$\begin{aligned} M_w &= -EC_S\eta_x', \\ M_t^P &= GI_t^P\theta_x', \\ M_t^S &= -GI_t^S\left(\eta_x - \theta_x\right), \end{aligned} \tag{10}$$

where

C_s, I_t^P, I_t^S are the warping, primary torsion, and secondary torsion constants, respectively, which are determined by:

$$\begin{aligned} C_S &= \int_\Omega \left(\phi_S^P\right)^2 d\Omega, \\ I_t^P &= \int_\Omega \left(y^2 + z^2 + y\frac{\partial \phi_S^P}{\partial z} - z\frac{\partial \phi_S^P}{\partial y}\right)d\Omega, \end{aligned} \tag{11}$$

$$I_t^S = k_x \int_\Omega \left[\left(\frac{\partial \phi_S^P}{\partial y}\right)^2 + \left(\frac{\partial \phi_S^P}{\partial z}\right)^2\right]d\Omega. \tag{12}$$

The transformations of Eqs. (9), (10), (11), and (12) are elucidated in detail, with a comprehensive explanation available in the work of Sapountzakis and Tsipiras (2010). It should be noted that Eq. (12) introduces the factor k_x, which is recognized as the torsion correction factor. Further insights into this factor can be found in Kim and Kim (2005), Murín and Kutiš (2008), and Mokos and Sapountzakis (2011).

The determination of the externally applied loading expressions m_t, m_w concerning the components of the traction vector, denoted t_x, t_y *and* t_z, is facilitated through the utilization of Eq. (8):

$$m_t(x) = \int_\Gamma \left(t_y(-z) + yt_z\right)ds,\ m_w(x) = -\int_\Gamma t_x\phi_S^P ds. \tag{13}$$

Upon substituting Eqs. (2), (3) and (6), (7), (9) for Eq. (8) and performing subsequent algebraic manipulations, the global equilibrium equations for the bar are derived as:

$$\begin{aligned} \frac{dM_t^P}{dx} + \frac{dM_t^S}{dx} &= -m_t, \\ \frac{dM_w}{dx} - M_t^S &= -m_w. \end{aligned} \tag{14}$$

By substituting Eq. (10) into Eq. (14), the global equilibrium equations are transformed into:

$$-G\left(I_t^P + I_t^S\right)\theta_x' + GI_t^S\eta_x' = m_t, \tag{15}$$

$$-EC_S\eta_x'' + GI_t^S\left(\eta_x - \theta_x'\right) = -m_w. \tag{16}$$

The longitudinal local equilibrium equation can be expressed as:

$$\begin{aligned} \frac{\partial \tau_{xy}^P}{\partial y} + \frac{\partial \tau_{xz}^P}{\partial z} &= 0, \\ \frac{\partial \sigma_{xx}}{\partial x} + \frac{\partial \tau_{xy}^S}{\partial y} + \frac{\partial \tau_{xz}^S}{\partial z} &= 0. \end{aligned} \tag{17}$$

It can be seen that the shear stress field in Eq. (7) does not guarantee an equilibrium, as stated in Eq. (17). Ferradi et al. (2013) assert that one warping mode cannot adequately address the challenge of a non-uniform torsion analysis. Genoese et al. (2013) employed a stress field independent of the displacement field for a non-uniform torsion problem. In response, Tsipiras and Sapountzakis (2014) introduced modifications to the shear stress field and introduced a warping mode, thereby correcting the stress field in Eq.(7) based on Eqs. (16) and (17) as follows:

$$\begin{aligned}\tau_{xy} = G\gamma_{xy} &= \underbrace{G\theta_x'\left(\frac{\partial\phi_S^P}{\partial y} - z\right)}_{\tau_{xy}^P} + \underbrace{\left[-G\left(\eta_x' - \theta_x'\right)\left(\frac{I_t^S}{C_S}\right)\right]\frac{\partial\phi_S^S}{\partial y}}_{\tau_{xy}^S},\\ \tau_{xz} = G\gamma_{xz} &= \underbrace{G\theta_x'\left(\frac{\partial\phi_S^P}{\partial y} + y\right)}_{\tau_{xz}^P} + \underbrace{\left[-G\left(\eta_x' - \theta_x'\right)\left(\frac{I_t^S}{C_S}\right)\right]\frac{\partial\phi_S^S}{\partial z}}_{\tau_{xz}^S},\end{aligned} \tag{18}$$

where, ϕ_S^S represents the secondary torsional warping function, corresponding to the shear center, which is denoted as S:

$$\begin{aligned}\nabla^2\phi_S^S &= \phi_S^P \text{ in } \Omega\\ \frac{\partial\phi_S^S}{\partial y}n_y + \frac{\partial\phi_S^S}{\partial z}n_z &= 0 \text{ on } \Gamma_n.\end{aligned} \tag{19}$$

The determination of k_x is grounded in an energy-based approach within elastic conditions, with detailed information available in Tsipiras and Sapountzakis (2012):

$$k_x = \frac{C_S^2}{\left(I_P - I_t^P\right)I_\phi}, \tag{20}$$

where

$$\begin{aligned}I_P &= \int_\Omega\left(y^2 + z^2\right)d\Omega,\\ I_\phi &= \iint_\Omega\left[\left(\frac{\partial\phi_S^S}{\partial y}\right)^2 + \left(\frac{\partial\phi_S^S}{\partial z}\right)^2\right]d\Omega.\end{aligned} \tag{21}$$

2.2 FEM procedures

2.2.1 For the angle of twist θ_x and torsion warping parameter η_x

By substituting Eqs. (6), (10) and (18) into the left hand of Eq. (8), the internal virtual work can be re-expressed as:

$$\begin{aligned}W_i = -EC_S\int_0^L \delta\left(\eta_x'\right)\left(\eta_x'\right)dx + GI_t^P\int_0^L \delta\left(\theta_x'\right)\theta_x' dx - GI_t^S\\ \int_0^L \delta\left(\eta_x - \theta_x'\right)\left(\eta_x - \theta_x'\right)dx.\end{aligned} \tag{22}$$

The virtual work done by external forces on the beam element, with the two end nodes, 1 and 2, can be explicitly expressed as:

$$\begin{aligned}W_e = \underbrace{\int_0^L\left(m_t(x)\delta\theta_x - m_w(x)\delta\eta_x\right)dx}_{Span} +\\ + \underbrace{\int_\Gamma\left(t_x\,\delta u + t_y\delta v + t_z\delta w\right)d\Gamma}_{end\ node,\ 1} + \underbrace{\int_\Gamma\left(t_x\,\delta u + t_y\delta v + t_z\delta w\right)d\Gamma}_{end\ node,\ 2}.\end{aligned} \tag{23}$$

By utilizing the formulations provided in Eqs. (2) and (13), the expression presented in Eq. (23) can be set out as:

$$\begin{aligned}W_e = \int_0^L m_t(x)\delta\theta_x dx - \int_0^L m_w(x)\delta\eta_x dx +\\ + \sum_{i=1}^{2}\widehat{m}_{ti}\delta\theta_{xi} - \sum_{i=1}^{2}\widehat{m}_{wi}\delta\eta_{xi}.\end{aligned} \tag{24}$$

To obtain the stiffness matrix of the beam element, interpolation of the independent variables θ_x and η_x within each element is necessary. The selection of shape functions for θ_x and H^0 is not limited due to their independence. For this study, the author utilized the 1D linear isoparametric shape function for both variables (Oñate, 2013):

$$\theta_x = \left[N_1(\xi) \quad N_2(\xi)\right]\begin{Bmatrix}\theta_{x1}\\ \theta_{x2}\end{Bmatrix}, \tag{25}$$

$$\eta_x = \left[N_1(\xi) \quad N_2(\xi)\right]\begin{Bmatrix}\eta_{x1}\\ \eta_{x2}\end{Bmatrix}, \tag{26}$$

where θ_{x1}, η_{x1}, θ_{x2}, η_{x2} are the degrees of the freedom of the two nodes of the element

$$N_1 = \tfrac{1}{2}(1-\xi),\ N_2 = \tfrac{1}{2}(1+\xi). \tag{27}$$

The nodal degrees of the freedom of the element associated with this approach can be expressed as:

$$\boldsymbol{d} = \{\theta_{x1}, \eta_{x1}, \theta_{x2}, \eta_{x2}\}^T. \tag{28}$$

By incorporating the expressions given by Eqs. (25) and (26) into Eqs. (22) and (24), one can obtain the element stiffness matrix and the element force vector as:

$$\boldsymbol{K}^e = \boldsymbol{K}_1^e + \boldsymbol{K}_2^e + \boldsymbol{K}_3^e, \tag{29}$$

$$\boldsymbol{F}^e = \boldsymbol{F}_1^2 - \boldsymbol{F}_2^e + \textstyle\sum_{i=1}^2 \boldsymbol{F}_{i(m_t)}^e - \sum_{i=1}^2 \boldsymbol{F}_{i(m_w)}^e, \tag{30}$$

where

$$\begin{aligned}\boldsymbol{K}_1^e &= -EC_S\int_{-1}^{1}\boldsymbol{B}_1^T\boldsymbol{B}_1 J d\xi = -EC_S\sum_i w_i\,\boldsymbol{B}_1^T(\xi_i)\boldsymbol{B}_1(\xi_i)J,\\ \boldsymbol{K}_2^e &= GI_t^P\int_{-1}^{1}\boldsymbol{B}_2^T\boldsymbol{B}_2 J d\xi = GI_t^P\sum_i w_i\,\boldsymbol{B}_2^T(\xi_i)\boldsymbol{B}_2(\xi_i)J,\\ \boldsymbol{K}_3^e &= -GI_t^S\int_{-1}^{1}\boldsymbol{B}_3^T\boldsymbol{B}_3 J d\xi = -GI_t^S\sum_i w_i\,\boldsymbol{B}_3^T(\xi_i)\boldsymbol{B}_3(\xi_i)J,\end{aligned} \tag{31}$$

$$\begin{aligned}\boldsymbol{F}_1^e &= \int_{-1}^{1} m_t\boldsymbol{N}_1^T J d\xi = \sum_i w_i\boldsymbol{N}_1^T(\xi_i)m_t J,\\ \boldsymbol{F}_2^e &= \int_{-1}^{1} m_w\boldsymbol{N}_2^T J d\xi = \sum_i w_i\boldsymbol{N}_2^T(\xi_i)m_w J,\end{aligned} \tag{32}$$

$F^e_{i(mt)}$ and $F^e_{i(mw)}$ are the nodal torsion moments and the warping moment at the end nodes i, respectively:

$$J = \frac{L}{2}, \tag{33}$$

$$\begin{aligned} \boldsymbol{B_1} &= [0 \quad N_{1,x} \quad 0 \quad N_{2,x}], \\ \boldsymbol{B_2} &= [N_{1,x} \quad 0 \quad N_{2,x} \quad 0], \\ \boldsymbol{B_3} &= [-N_{1,x} \quad N_1 \quad -N_{2,x} \quad N_2], \end{aligned} \tag{34}$$

$$\begin{aligned} \boldsymbol{N_1} &= [N_1 \quad 0 \quad N_2 \quad 0], \\ \boldsymbol{N_2} &= [0 \quad N_1 \quad 0 \quad N_2], \end{aligned} \tag{35}$$

The weights and integration points of the Gaussian integration technique are represented by w_i and ξ_i, respectively. To avoid shear locking in the current investigation, a one-point Gauss quadrature with $w_i = 0$, $\xi_i = 0$ is employed. The equation for the system matrix for assembling the element stiffness ma-trix and load vectors is given below:

$$\boldsymbol{K}.\boldsymbol{d} = \boldsymbol{F}. \tag{36}$$

2.2.2 Warping function, ϕ^P_S, ϕ^S_S

By applying Galerkin's method and using the test function $\eta \in H^1(\Omega)$ along with the Gauss-Green theorem, the governing Eqs. (2) and (19) can be transformed into a weak form as follows:

$$\begin{aligned} G(\phi^P_S,\eta) = & \int_\Omega \left(\frac{\partial \phi^P_S}{\partial y}\frac{\partial \eta}{\partial y} + \frac{\partial \phi^P_S}{\partial z}\frac{\partial \eta}{\partial z} \right) d\Omega \ - \\ & - \oint_{\Gamma_n} \left(n_y z - n_z y \right) \eta ds = 0, \end{aligned} \tag{37}$$

$$\begin{aligned} G(\phi^S_S,\eta) = & \int_\Omega \left(\frac{\partial \phi^S_S}{\partial y}\frac{\partial \eta}{\partial y} + \frac{\partial \phi^S_S}{\partial z}\frac{\partial \eta}{\partial z} \right) d\Omega \ - \\ & - \int_\Omega \left(-\phi^P_S \eta \right) d\Omega = 0. \end{aligned} \tag{38}$$

The FEM is utilized to approximate the values of the warping function, ϕ^P_S, and ϕ^S_S, in Eqs. (37) and (38), as outlined in previous works (Tran et al., 2021).

3 NUMERICAL RESULTS AND DISCUSSION

This section evaluates the accuracy of the proposed FEM, which considers a shear deformation analysis in non-uniform torsion. The formulations presented in the previous sections provide the framework for a software program called RWT, which was implemented using MATLAB R2015a. The program examined thin-walled beams with open and closed cross-sections under different boundary and loading conditions. Ultimately, the results were compared to those of previous field studies to verify the proposed approach's validity.

3.1 Example 1

In the first example, an analysis was conducted on a cantilevered thin-walled beam with a channel cross-section, as illustrated in Fig. 2. The beam has a length of $L = 18$ m and is composed of a material with a modulus of elasticity $E = 30$ MPa and a Poisson ratio of $v = 0.154$. The thin-walled beam of interest is acted upon by a concentrated torsional moment, which has a value of $M_x = 1000$ kN.m, at its tip. To evaluate the accuracy of the proposed method, this case was analyzed using the RWT computer code. Specifically, 600 axial elements and 60 elements in the cross-section were utilized in the analysis. The RWT-based determination yields the following values for the geometric constants of the cross-section: $I^P_t = 0.0320$ m^4, $I^S_t = 7.4241$ m^4, and $C_S = 14.1770$ m^6. The boundary conditions at the clamped left end are specified as $\theta_x = \eta_x = 0$.

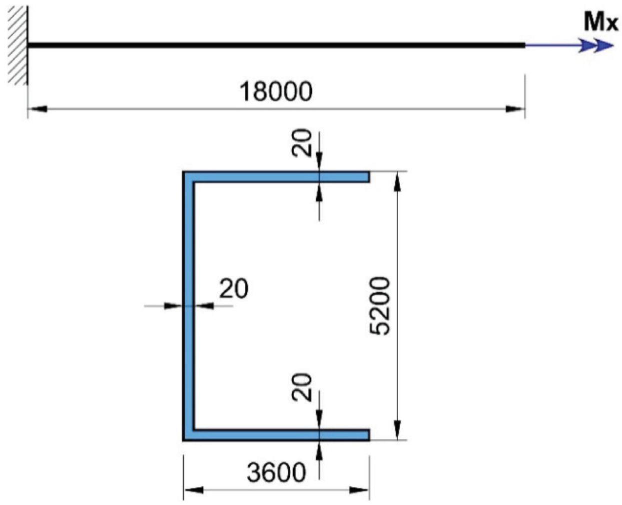

Fig. 2 *A cantilevered beam with a channel cross-section and an applied load, with all the dimensions expressed in millimeters*

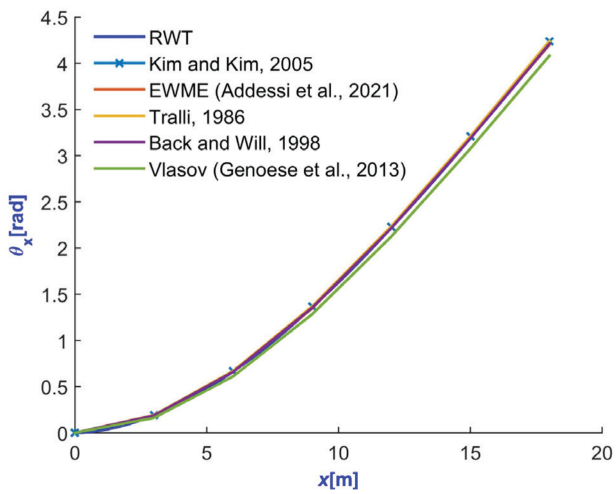

Fig. 3 *The twist angle along the x-axis of the beam in ex. 1*

Tab. 1 shows the twist angle at the free end obtained from the proposed method and compared with the values reported in previous works, such as Tralli (1986), Back and Will (1998), Kim and Kim (2005), Genoese et al. (2013), and Addessi et al. (2021). The comparison between the twist angle at the free end obtained from the RWT analysis and the results of the FEM 3D-Solid (Genoese et al. 2013) reveals good agreement, as shown in Tab. 1. Fig. 3 illustrates the changes in the twist angle over the length of the beam; these results were compared with the findings from previous studies (Tralli, 1986; Back and Will, 1998; Kim and Kim, 2005; Genoese et al., 2013; Addessi et al., 2021). Notably, the RWT method demonstrates a high level of agreement with the approaches that account for the shear deformation effects.

Tab. 1 *Comparison of the twist angle θ_x at the free end between the methods*

Methods	θ_x[rad] at $x = L$
RWT	4.2098
Tralli, 1986	4.239
Back and Will, 1998	4.21
Kim and Kim, 2005	4.236
Vlasov (Genoese et al., 2013)	4.081
Benscoter type (Genoese et al., 2013)	4.139
Jourawsky type (Genoese et al., 2013)	4.211
3D-Solid (Genoese et al., 2013)	4.210
3D-Plate (Genoese et al., 2013)	4.235
Saint-Venant model (Genoese et al., 2013)	43.373
EWME (Addessi et al., 2021)	4.2

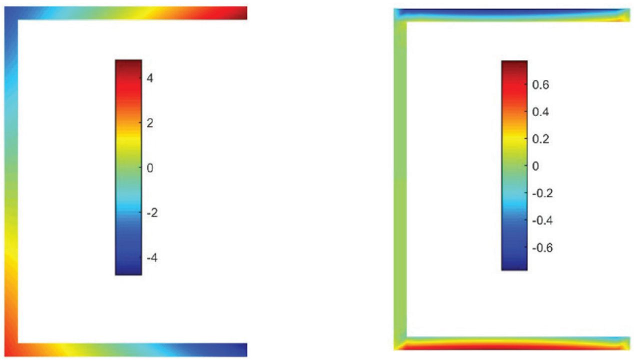

(a) (b)

Fig. 4 *a) The normal stress σ_{xx} and b) the shear stress τ_{xy} at x = 4.5 m from the fixed support units [MPa]*

Fig. 4 presents the depiction of the distribution of the axial stress σ_{xx} and shear stress τ_{xy} within the channel cross-section. The peak normal stress of σ_{xx} = 4.7911 MPa is observed at the flange tip. The distribution of shear stress τ_{xy}, with a maximum value of 0.7721 MPa exhibits a decreasing trend from the outer flange edge towards the inner edge. Based on the observations from Fig. 4, it can be noted that the results obtained by RWT are consistent with those documented by (Genoese et al., 2013; Addessi et al., 2021).

3.2 Example 2

In this section, we will investigate the behavior of a cantilevered thin-walled beam having a box-shaped cross-section. The dimensions of the beam are depicted in Fig. 5. The beam is made of a material with a modulus of elasticity E = 2x10^5 MPa and a Poisson's ratio of v = 0.3. A uniformly distributed

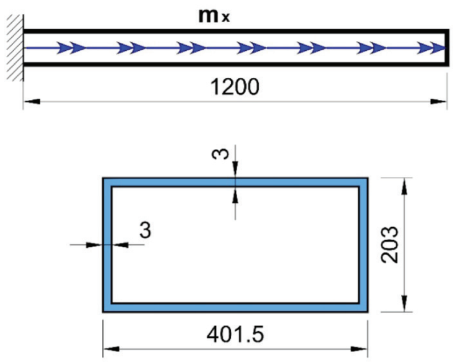

Fig. 5 *A cantilevered beam with a box cross-section and the applied load, with all the dimensions expressed in millimeters*

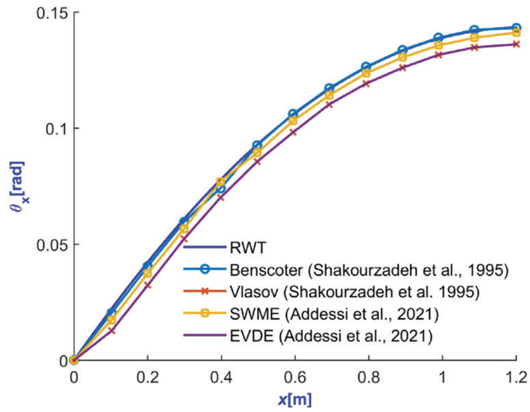

Fig. 6 *The twist angle along the x-axis of the cantilever beam in ex. 2*

twisting moment with a magnitude of m_x = 1000 kN.m/m was applied to the thin-walled beam under consideration. To investigate the beam, a RWT with 600 axial elements and 394 cross-sectional elements was employed. The geometric constants of the cross-section, as obtained through computations, are as follows: I^P_t = 6.39867 x 10^{-5} m^4, I^S_t = 6.1784 x 10^{-6} m^4; C_S = 5.3314 x 10^{-8} m^6. The boundary conditions at the clamped left end are specified as $\theta_x = 0$, $\eta_x = 0$.

Shakourzadeh et al. (1995) utilized FEM with Benscoter's model to analyze the problem and compared their results with those obtained from the Vlasov's theory, which ignores shear deformation. On the other hand, Addessi et al. (2021) employed two distinct models, i.e., EVDE and SWME, to comprehensively analyze the global and local aspects of the problem. EVDE is an improved version of the Vlasov's model, while SWME is a simplified method based on Benscoter's theory.

Fig. 6 presents the variations of the twist angle θ_x, while Figs. 10a and 10b illustrate the torsion warping parameter η_x and bi-moment M_w (warping moment) along the length of the thin-walled beam with respect to the different methods used for the analysis. The results indicate that the outcomes obtained from RWT are consistent with those of FEM as proposed by Shakourzadeh et al. (1995), which utilized Benscoter's beam theory. Notably, the latter method provides remarkably precise results under torsional loading conditions.

Concerning the bi-moment, variations were observed among the outcomes of the various models in the vicinity of the fixed support. In particular, the significant discrepan-

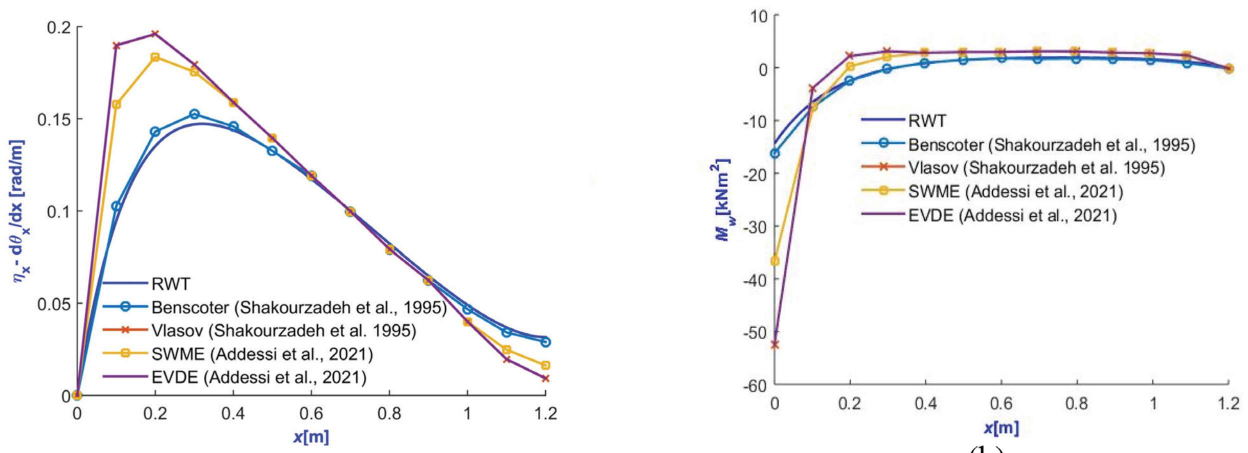

(a) (b)

Fig. 7 *The variations along the length of the beam of a) torsion warping parameter η_x - $d\theta_x/dx$ [rad/m] b) bimoment M_w [kN.m^2]*

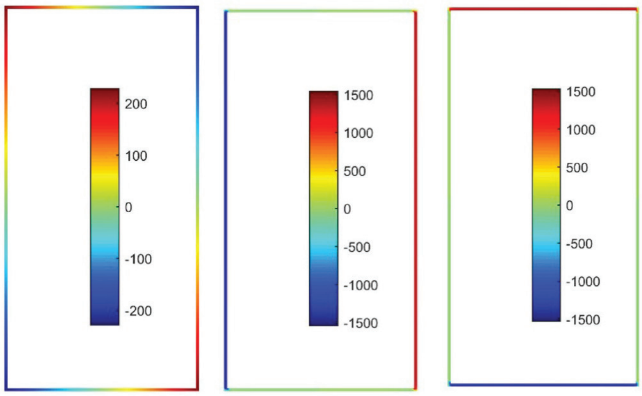

(a) (b) (c)

Fig. 8 *The 2D cross-section stress distribution at 0.1m from the fixed end a) axial stress σ_{xx}, and shear stress b) τ_{xy}, c) τ_{xz} (units MPa)*

cy between the findings of Shakourzadeh et al. (1995) and RWT compared to other models near the support is primarily due to the impact of the shear deformation effect, which was not accounted for in Vlasov's model. Nevertheless, the methods exhibit good agreement at distances away from the fixed end.

The distributions of the stress components across the cross-section, which are located 0.1m from the fixed end, are illustrated in Fig. 8. The maximum normal stress value of the box-section beam predicted by RWT is 858.4 MPa. In comparison, the theoretical model of Shakourzadeh et al. (1995) reports this value as 866.36 MPa. The hypothesis presented in the literature regarding the torsion of thin-walled beams with closed cross-sections (Saad et al., 2004) suggests that the shear stresses are uniformly distributed throughout the thickness of a beam. This phenomenon is accurately captured by RWT.

3.3 Example 3

The third case study involves a thin-walled cantilever beam with a box cross-section, as depicted in Fig. 9. The beam's dimensions are L = 0.95 m, and the beam is made of a material with a modulus of elasticity E = 79x10^3 MPa and a shear modulus G = 31.102 x10^3 MPa. A concentrated torsional moment M_x = 0.1 kN.m was applied at a distance of 0.8 m from the fixed end. To analyze this example, RWT was employed using a finite element model consisting of 56 axial elements and 304 elements in the cross-section. The RWT yielded the following geometric constants of the cross-section: I_t^P = 5.89808 x 10^{-8} m^4, I_t^S = 1.6763 x 10^{-8} m^4, C_S = 2.1357 x 10^{-12} m^6. The boundary conditions at the clamped left end are specified as $\theta_x = 0$, $\eta_x = 0$.

Murín et al. (2012, 2014) conducted a FEM analysis of the problem, taking into account the secondary warping effect. It is worth noting that this example has undergone experimental verification. The variations of the twist angle along the length of the beam are presented in Fig. 10 and are compared with the results obtained from i) the 14 x 14 stiffness matrix, including the secondary torsional moment deformation effect (STMDE); ii) the ANSYS commercial software, which employed either the BEAM 188 element (with warping freedom) or shell model (using SHELL 181), and iii) the experimental measurements. Furthermore, Tab. 2 provides the values of the twist angle at various positions along x, which are compared with those obtained from (Murín et al., 2012; Murín et al., 2014).

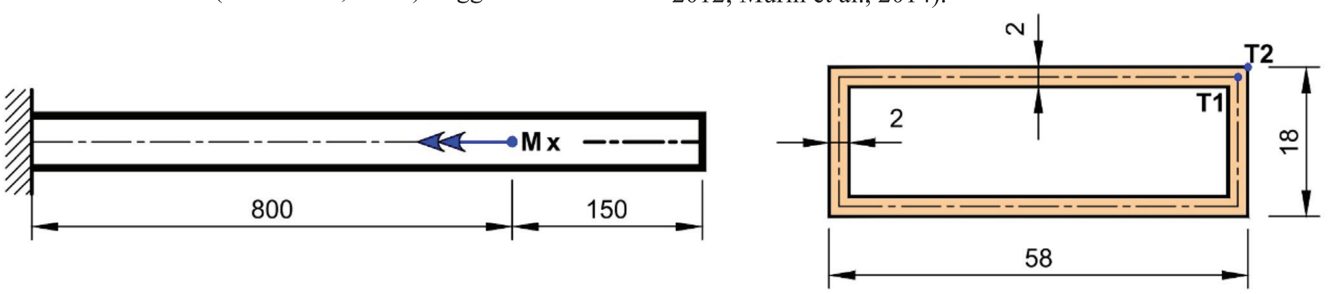

Fig. 9 *A cantilever beam, the load applied, and the geometry of the cross-section, units [mm]*

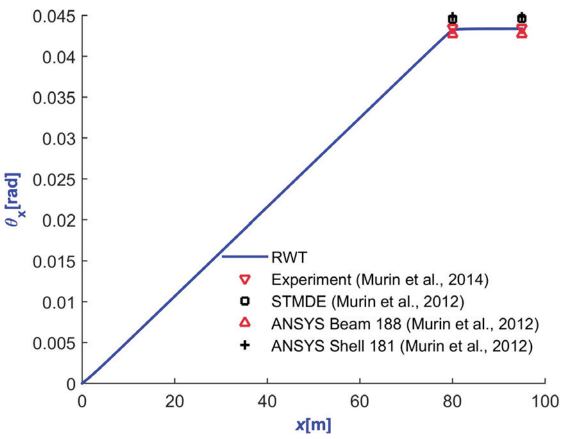

Fig. 10 *Angle of twist along the axis x of the cantilever beam in ex. 3*

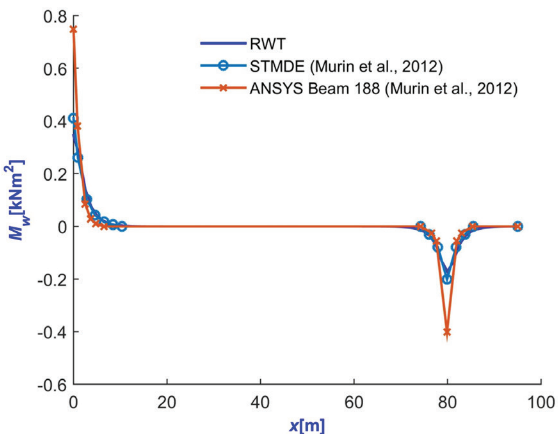

Fig. 11 *The variations along the length of the beam of bi-moment M_w*

Fig. 10 presents the variations of the bi-moment along the length of the beam, which are compared to those obtained from (Murín et al., 2012; Murín et al., 2014) using i) the 14 x 14 stiffness matrix including STMDE and ii) the ANSYS commercial software employing the BEAM 188 element. The results obtained by RWT for the bi-moment are in good agreement with the results of STMDE (Murin et al., 2012). Notably, the ANSYS software results for the BEAM 188 element show a considerable error. Additionally, Tab. 3 provides the values of the axial stress at various x positions compared to those retrieved from (Murín et al., 2012; Murín et al., 2014). It is important to note that point T1 is situated on the mid-line of the cross-section, while T2 refers to the upper boundary curve of the cross-section. The consistency of the results obtained from RWT with those obtained from the literature in both the figures and tables demonstrates the reliability of RWT.

Tab. 2 *Comparison angle of twist θ_x [rad] between the methods*

Methods	x = 80 cm	x = 95 cm
RWT	0.0432	0.0434
STMDE (Murín et al., 2012)	0.0433	0.0434
ANSYS Beam 188 (Murín et al., 2012)	0.0428	0.0430
ANYSYS Shell 181 (Murín et al., 2012)	0.0448	0.0449
Experiment data (Murín et al., 2014)	0.0435	-

3.4 Example 4

For the fourth example, a continuous thin-walled beam with a closed-box cross-section was analyzed using RWT with 544 axial elements and 124 elements in the cross-section. In Fig. 12, the beam's geometry is presented; a concentrated moment M_x = 30 kN.m is applied at x = 2 and 7.5 m. The modulus of elasticity is E = 21 x 10^5 MPa, and the Poisson ratio is v = 0.3125. The RWT analysis yielded the following geometric constants: I_t^P = 0.0915 m^4, I_t^S = 0.0014 m^4, and C_S= 2.3031 x 10^{-4} m^6. The boundary condition at the node corresponding with the simple supports is specified as $\theta_x = 0$.

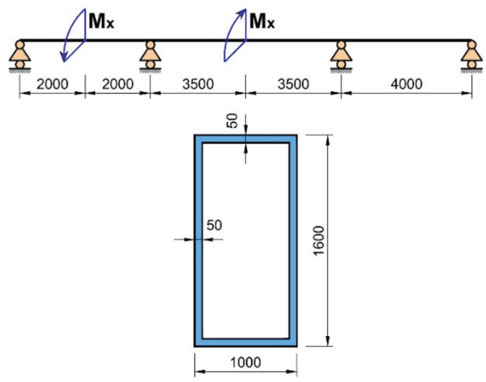

Fig. 12 *Schematic representation of a continuous beam subjected to an applied load, along with the cross-sectional geometry (millimeters)*

Tab. 3 *Comparison of the axial stress at various positions between the methods, unit [MPa]*

Positions [mm]	Experiment data (Murín et al., 2014)	STMDE (Murín et al., 2012)	ANSYS Beam 188 (Murín et al., 2012)	RWT (T1)	RWT (T2)
3	25.11	25.87	56.56	24.5272	29.0682
11	18.55	18.12	25.31	17.8979	21.2115
19	12.24	11.97	12.34	11.1121	13.1694
794	10.65	11.19	18.67	10.9245	12.9471
800	12.52	14.53	29.05	11.8923	14.0941
950	2.49	0.185	-	0.0056	0.0066

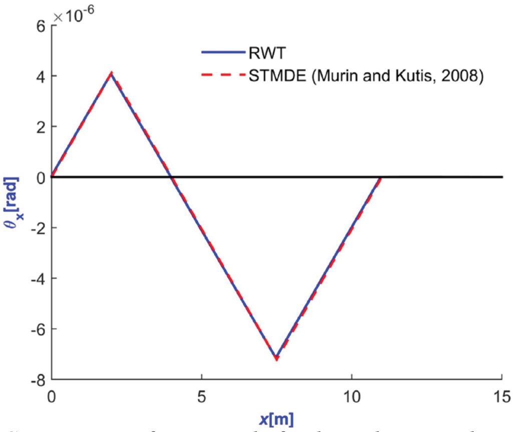

Fig. 13 *Comparison of twist angle θ_x along the axis x between the methods*

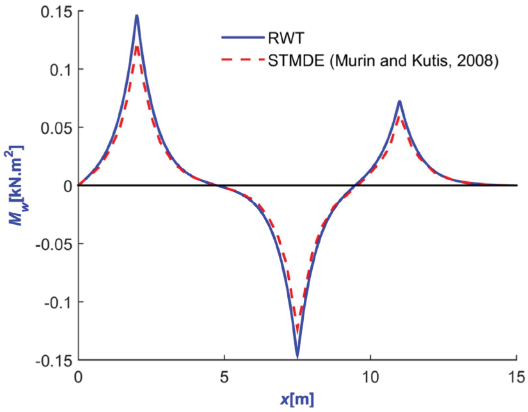

Fig. 14 *The variations along the beam length of the bi-moment M_w*

This test was also investigated in the reports of (Murín and Kutiš, 2008; Genoese et al., 2013). In (Murín and Kutiš, 2008), a 14 x 14 stiffness matrix, including the shear deformation effect, was developed. Genoese et al. (2013) presented two models for non-uniform torsion, which they identified as the Jaurawsky model and the Benscoter model. The comparison between the variations of the angle twist along the length of the beam obtained from RWT and STMDE (Murín and Kutiš, 2008) is shown in Fig. 13. The twist angle values at various x positions are presented in Tab. 4 and compared with the results reported in (Murín and Kutiš, 2008; Genoese et al., 2013). It is noteworthy that the twist angle results obtained by RWT demonstrate convergence with those from Genoese et al.'s Jaurawsky model and the FEM solid model (Genoese et al., 2013), as shown in Tab. 4.

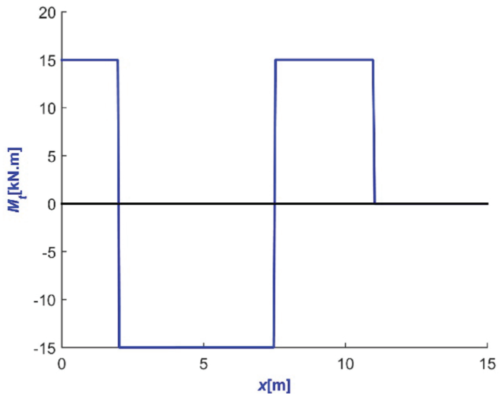

Fig. 15 *The variations along the beam length of the total twisting moment M_t*

Tab. 4 *Comparison angle of twist $\theta_x \times 10^{-6}$ [rad]*

Methods	x = 2 m	x = 7.5 m
RWT	4.0784	-7.1462
STMDE (Murín and Kutiš, 2008)	4.1200	-7.2100
ANSYS Beam 188 (Murín and Kutiš, 2008)	3.93	-6.92
Jaurawsky model (Genoese et al., 2013)	4.084	-7.1560
Benscoter model (Genoese et al., 2013)	4.0110	-7.0660
FEM solid model (Genoese et al., 2013)	4.0990	-7.1620
FEM shell model (Genoese et al., 2013)	4.1230	-7.2430
Saint Venant solution (Genoese et al., 2013)	4.1040	-7.1880

Tab. 5 *Bi-moment M_w [kN.m^2] at the various positions*

Methods	x = 2 m	x = 7.5 m	x = 11 m
RWT	0.1458	-0.1458	0.0727
STMDE (Murín and Kutiš, 2008)	0.1234	-0.1234	0.06125
ANSYS Beam 188 (Murín and Kutiš, 2008)	0.856	-0.805	-

Fig. 14 depicts the variation of the bi-moment along the length of the beam and compares it to the results obtained from Murín and Kutiš (2008), as well as those obtained using the 14 x 14 stiffness matrix and the ANSYS commercial software employing the BEAM 188 element.

In Tab. 5, the values of the bi-moment's various x positions are also compared to the ones retrieved from (Murín and Kutiš, 2008). The accuracy of RWT can be verified from Fig. 14 and Tab. 5. The variations of the total twisting moment along the length of the beam presented in Figure 18 are in accordance with the results obtained in (Murín and Kutiš, 2008).

4 CONCLUSIONS

The primary aim of this research was not to propose new theories but to apply established theoretical frameworks to develop numerical methodologies using finite elements for problem-solving. This study employs the FEM referred to as RWT to meticulously address the complexities of non-uniform torsion. It also integrates shear deformation and warping in thin-walled beams with a consistently arbitrary cross-section composed of homogeneous isotropic material throughout their length. The warping function is deduced using Galerkin's method applied to elliptical differential equations. A one-dimensional FEM application yields two independent variables, specifically the twist angle and torsion warping parameter.

The precision of RWT is corroborated through numerical examples, thereby producing results that concur with the extant literature and corroborate Benscoter's theory. The empirical evidence further highlights RWT's accuracy in predicting thin-walled beam behavior under non-uniform torsion, which underscores its practical relevance in design applications. The proposed method's efficacy, including the shear deformation and warping, is in harmony with contemporary trends.

Despite the potential of the BEM of Tsipiras and Sapountzakis' (2014), practical limitations persist, with significant software companies still favoring FEM. The author's two-dimensional FEM, which employs the Galerkin approach and aligns with prevalent industry standards, emerges as a viable solution for effectively addressing non-uniform torsion in thin-walled beams. This approach is compatible with commercial software applications such as IDEA StatiCa, SCAD, and AllPlan Bridge.

In summary, this research substantiates and validates the theoretical framework proposed by Tsipiras and Sapountzakis (2014). By employing FEM, the study conducts a thorough examination of non-uniform torsion calculations in thin-walled beams and presents a significant application of FEM concerning the issue of non-uniform torsion. The exploration of practical implications illustrates the applicability of the theoretical framework in tangible engineering scenarios. The study works to pave the way for further research and advances, validates existing theoretical frameworks, and enhances the understanding of non-uniform torsion in thin-walled beams.

REFERENCES

Addessi, D. – Di Re, P. – Cimarello, G. (2021) *Enriched beam finite element models with torsion and shear warping for the analysis of thin-walled structures*, Thin-Walled Structures, vol. 159. DOI:10.1016/j.tws.2020.107259.

Allplan Bridge - Software for Bridge Engineering. Retrieved Jan 28, 2024, from https://www.allplan.com/products/allplan-bridge/

Back, S.Y. – Will, K. M. (1998) *A shear-flexible element with warping for thin-walled open beams,* International Journal for Numerical Methods in Engineering,vol. 43, No. 7, pp. 1173–1191. DOI:10.1002/(SICI)1097-0207(19981215)43:7<1173::AID-NME340>3.0.CO;2-4.

Benscoter, S. U. (1954) *A Theory of Torsion Bending for Multicell Beams,* Journal of Applied Mechanics, vol. 21, No. 1, pp. 25–34. DOI:10.1115/1.4010814.

Braess, D. (2007) *Finite Elements. Theory, Fast Solvers, and Applications in Elasticity Theory*, 3rd ed, Cambridge University Press.

El Fatmi, R. (2007) *Nonuniform warping including the effects of torsion and shear forces*, *Part I: A general beam theory*, International Journal of Solids and Structures, vol. 44, Nos. 18–19. pp. 5912–5929. DOI:10.1016/j.ijsolstr.2007.02.006.

El Fatmi, R. (2007) *Nonuniform warping including the effects of torsion and shear forces. Part II: Analytical and numerical applications,* International Journal of Solids and Structures, vol. 44, Nos. 18–19, pp. 5930–5952. DOI:10.1016/j.ijsolstr.2007.02.005.

Erkmen, R. E. – Mohareb, M. (2006) *Torsion analysis of thin-walled beams including shear deformation effects,* Thin-walled structures, vol. 44, No. 10, pp. 1096–1108. DOI:10.1016/j.tws.2006.10.012.

Ferradi, M. K. – Cespedes, X. – Arquier, M. (2013) *A higher order beam finite element with warping eigenmodes,* Engineering Structures, vol. 46, pp. 748–762. DOI:10.1016/j.engstruct.2012.07.038.

Fialko, S. Y. – Lumelskyy, D.E. (2013) *On numerical realization of the problem of torsion and bending of prismatic bars of arbitrary cross section*. J Math Sci, vol. 192, pp. 664–681. DOI: 10.1007/s10958-013-1424-4.

Genoese, A., Genoese, A., Bilotta, A., & Garcea, G. **(2013)**. *A mixed beam model with nonuniform warpings derived from the Saint Venànt rod*, Computers & Structures, vol. 121, pp. 87-98. DOI:10.1016/j.compstruc.2013.03.017

Gruttmann, F. – Sauer, R. – Wagner, W. (1999) *Shear stresses in prismatic beams with arbitrary cross-sections*, International Journal for Numerical Methods in Engineering, vol. 45, No. 7, pp. 865–889. DOI:10.1002/(SICI)1097-0207(19990710)45:7<865::AID-NME609>3.0.CO;2-3.

IDEA StatiCa - Structural Engineering Software. Retrieved Jan 28, 2024, from https://www.ideastatica.com/

Kim, N. I. – Kim, M.Y. (2005) *Exact dynamic/static stiffness matrices of non-symmetric thin-walled beams considering coupled shear deformation effects*, Thin-Walled Structures, vol. 43, No. 5, pp. 701–734. DOI:10.1016/j.tws.2005.01.004.

Kugler, S. – Fotiu, P.A. – Murín, J. (2021). *A novel GBT-formulation for thin-walled FGM-beam-structures based on a reference beam problem*. Composite Structures, vol. 257. DOI: 10.1016/j.compstruct.2020.113158.

Lewiński, T. – Czarnecki, S. (2021) *On incorporating warping effects due to transverse shear and torsion into the theories of straight elastic bars*, Acta Mechanica, vol. 232, pp. 247–282. DOI:10.1007/s00707-020-02849-7.

Librescu, L. – Song, O. (2005) *Thin-walled composite beams: theory and application*, vol. 131, Springer Science & Business Media.

Mokos, V. G., & Sapountzakis, E. J. (2011) *Secondary torsional moment deformation effect by BEM,* International Journal of Mechanical Sciences, vol. 53, No. 10, pp. 897-909. DOI: 10.1016/j.ijmecsci.2011.08.001.

Murín, J. – Aminbaghai, M. – Kutiš, V. – Královič, V. – Sedlár, T. – Goga, V. – Mang, H. (2014) *A new 3D Timoshenko finite beam element including nonuniform torsion of open and closed cross sections*, Engineering Structures, vol. 59, pp. 153–160. DOI:10.1016/j.engstruct.2013.10.036.

Murin, J. – Kugler, S. – Hrabovsky, J. – Kutis, V. – Paulech, J. – Aminbaghai, M. (2021). *Influence of spatially varying material properties on the bimoment normal and shear stresses by warping torsion of FGM beams*, Composite Structures, vol. 256, DOI: 10.1016/j.compstruct.2020.113043.

Murín, J. – Kugler, S. – Hrabovsky, J. – Kutiš, V. – Paulech, J. – & Aminbaghai, M. (2022). *Warping torsion of FGM beams with spatially varying material properties*. Composite Structures, vol. 291. DOI: 10.1016/j.compstruct.2022.115592.

Murín, J. – Kutiš, V. – Královič, V. – Sedlár, T. (2012) *3D beam finite element including nonuniform torsion*, Procedia Engineering, vol. 48, pp. 436–444. DOI:10.1016/j.proeng.2012.09.537.

Murín, J. – Kutiš, V. (2008) *An effective finite element for torsion of constant cross-sections including warping with secondary torsion moment deformation effect*, Engineering Structures,vol. 30, No. 10, pp. 2716–2723. DOI:10.1016/j.engstruct.2008.03.004.

Oñate, E. (2013) *Structural analysis with the finite element method. Linear statics: volume 2: beams, plates and shells.* Springer Science & Business Media.

Paradiso, M. – Vaiana, N. – Sessa, S. – Marmo, F. – Rosati, L. (2020) *A BEM approach to the evaluation of warping functions in the Saint Venant theory*, Engineering Analysis with Boundary Elements, vol. 113, pp. 359–371. DOI:10.1016/j.enganabound.2020.01.004.

Pilkey, W. D. (2002) *Analysis and design of elastic beams: Computational methods*, John Wiley & Sons.

Prokić, A. (1993) *Thin-walled beams with open and closed cross-sections*, Computers and Structures, vol. 47, No. 6, pp. 1065–1070. DOI:10.1016/0045-7949(93)90310-A.

Prokić, A. (1996) *New warping function for thin-walled beams. II: Finite element method and applications*. Journal of Structural Engineering, vol. 122, No. 12, pp. 1443–1452. DOI: 10.1061/(ASCE)0733-9445(1996)122:12(1443).

Saadé, K. – Espion, B. – Warzée, G. (2004) *Nonuniform torsional behavior and stability of thin-walled elastic beams with arbitrary cross sections*, Thin-Walled Structures, vol. 42, No. 6, pp. 857–881. DOI:10.1016/j.tws.2003.12.003.

SAP2000 Structural analysis and design. Computers and Structures, Inc. (n.d.). Retrieved May 15, 2022, from https://www.csiamerica.com/products/sap2000.

Sapountzakis, E. J., & Tsipiras, V. J. (2010). *Shear deformable bars of doubly symmetrical cross section under nonlinear nonuniform torsional vibrations—application to torsional postbuckling configurations and primary resonance excitations*, Nonlinear Dynamics, vol. 62, pp. 967-987. DOI: 10.1007/s11071-010-9778-3.

SCAD Software - Structural Analysis and Design. Retrieved Jan 28, 2024, from https://scadsoft.com/en

SCIA English Homepage. SCIA Structural Analysis Software and Design Tools. Retrieved 16 Jan 2022, from https://www.scia.net/en.

Shakourzadeh, H. – Guo, Y. Q. – Batoz, J.L. (1995) *A torsion bending element for thin-walled beams with open and closed cross sections*, Computers and Structures, vol. 55, No. 6, pp. 1045–1054. DOI:10.1016/0045-7949(94)00509-2.

Timoshenko, S. P. – Goodier, J. N. (1970) *Theory of Elasticity*, 3rd ed, McGraw-Hill Book Co.

Timoshenko, S. P. X. (1922) *On the transverse vibrations of bars of uniform cross-section*, The London, Edinburgh, and Dublin Philosophical Magazine and Journal of Science, vol. 43, No. 253, pp. 125–131. DOI:10.1080/14786442208633855.

Timoshenko, S. P. LXVI. (1921) *On the correction for shear of the differential equation for transverse vibrations of prismatic bars*, The London, Edinburgh, and Dublin Philosophical Magazine and Journal of Science, vol. 41, No. 245, pp. 744–746. DOI:10.1080/14786442108636264.

Tralli, A. (1986) *A simple hybrid model for torsion and flexure of thin-walled beams*, Computers and Structures, vol. 22, No. 4, pp. 649–658. DOI:10.1016/0045-7949(86)90017-9.

Tran, D. B. – Navrátil, J. – Čermák, M. (2021) *An efficiency method for assessment of shear stress in prismatic beams with arbitrary cross-sections*, Sustainability (Switzerland), vol. 13, No. 2. pp. 1–20. DOI:10.3390/su13020687.

Tran, D. B. (2021) *Torsional Shear Stress in Prismatic Beams With Arbitrary Cross-Sections Using Finite Element Method,* Stavební obzor - Civil Engineering Journal, vol. 30, No. 2. DOI:10.14311/cej.2021.02.0030.

Tsipiras, V. J. – Sapountzakis, E. J. (2014). *Bars under nonuniform torsion–Application to steel bars, assessment of EC3 guidelines*. Engineering structures, vol. 60, pp.133-147. DOI: 10.1016/j.engstruct.2013.12.027.

Tsipiras, V. J. – Sapountzakis, E.J. (2012) *Secondary torsional moment deformation effect in inelastic nonuniform torsion of bars of doubly symmetric cross section by BEM*, International Journal of Non-Linear Mechanics, vol. 47, No. 4, pp. 68–84. DOI: 10.1016/j.ijnonlinmec.2012.03.007.

Vlasov, V. Z. (1961) *Thin walled elastic beams*, Israel Program for Scientific Translations, Jerusalem, Israel.

Wunderlich, W. – Pilkey, W.D. (2002) *Mechanics of structures: variational and computational methods*, 2d ed. CRC Press, 912 pp.

Zienkiewicz, O. C. – Taylor, R. L. (2000) *The finite element method: the basis,* vol.1, 5th ed. Butterworth-Heineman.